The Response of Polarization Maintaining Fibers upon Temperature Field Disturbance

Filip DVORAK[1], *Jan MASCHKE*[2], *Cestmir VLCEK*[2]

[1]Department of radar technology, Faculty of Military Technology, University of Defence, Kounicova 65, Brno, 602 00, Czech Republic
[2]Department of electrical engineering, Faculty of Military Technology, University of Defence, Kounicova 65, Brno, 602 00, Czech Republic

filip.dvorak@unob.cz, jan.maschke@email.cz, cestmir.vlcek@unob.cz

Abstract. *The paper deals with the response of polarization maintaining (PM) fibers upon the variation of the temperature field, on condition both polarization axes are excited. Proper use can be applied in the area of optical fiber thermal field disturbance sensor. For a description of polarization properties the coherent Jones and Muller matrices were used. The Poincare sphere was applied to depict the development of the output of the polarization state of PM fibers for wavelengths 633 nm, 1310 nm and 1550 nm were arranged in a proposed sensor setup and were studied in the laboratory. A wide file of results containing dependencies of phase shift variations upon different configurations of measured PM fiber was obtained. The thermal field disturbance of the PM fiber was applied by an object with defined proportions and a defined range of temperatures. Dependencies of phase shift upon the object's temperature, its distance from the fiber and exposed length of PM fiber were measured.*

Keywords

Beat length, coherency matrix, fiber response, Poincare sphere, sensor, state of polarization.

1. Introduction

From the beginning of fiber realization in the telecommunications area it got to the big development of the theory and practical applications. Almost in the same time there were ideas on the application of fibers also in sensors. Isotropic fibers [1], polarization maintaining fibers (PMF) and rare earth doped fibers [2] have been used in the number of sensor applications. One example of an application is the interferometric sensor of gyroscope [3], [4]. Polarization maintaining fibers were established for exciting of optical radiation to one polarization axis only and maintenance polarization state along the whole length of the fiber. According to the induced birefringence, fibers were applied in sensors, e.g. for measurement of mechanical pressure [5].

The artificial birefringence caused by the different thermal expansibility between strength elements and the fiber cladding reaches high sensitivity to the ambient temperature of surrounding environment [6]. For uniform excitation of both fiber axes there is a polarization state change of optical radiation in the fiber output caused by the ambient thermal field disturbance. The change of the polarization state of output optical radiation immediately detects any thermal field disturbance caused by an ambient thermal source. High fiber sensitivity to the outer thermal field initiated the idea to use the PMF application as a sensor of thermal field disturbance.

Infant of the research work, time development of output polarization fluctuation in PANDA PMF and bowtie for equal excitation of both polarization axes were studied. Expressive fluctuation led to the construction of a fiber sensor realized and evaluated for $\lambda = 633$ nm, utilizing good polarization properties of He-Ne laser. The measured results validated high sensor sensitivity upon the external thermal field. The disadvantage of this sensor is its construction arrangement using gas He-Ne laser as a source of optical radiation. To eliminate this disadvantage and to compare different properties of the components used, the experiment was extended for PANDA PM fibers and semiconductor lasers with wavelengths of 1550 nm and 1310 nm wavelengths.

Results of theoretical analysis and partial experimental tests for $\lambda = 633$ nm and 1550 nm were published in previous papers [7], [8], [9], [10]. Two partial experiments for $\lambda = 1550$ nm have been made there. The rate of fiber response depending upon the distance between external thermal source and the fiber

was studied in the first one. Effects of PMF response to its exposed length were studied in the second one. Presented work is an extension of previous experiments for a wavelength of 1310 nm. This work focuses mainly on the determination of fiber response in both dependences during an excitation by an external thermal field with variable initial temperature. All the results obtained for the three particular PM fibers will be compared.

2. Principle of Sensor Function

The part of PMF can be, in principle, studied as a multiple linear retarder containing no partial polarizers and can be described by means of a unitary Jones matrix. Output optical radiation from the PMF can be described by coherency matrix $\mathbf{C}'$, that is determined by the unitary Jones matrix of the given component $\mathbf{L}$ and also by a coherency matrix of input optical radiation $\mathbf{C}$ according to: [11]

$$\begin{aligned}\mathbf{C}' &= (\mathbf{LE}) \otimes (\mathbf{LE})^{+} = (\mathbf{LE}) \otimes (\mathbf{L}^{+}\mathbf{E}^{+}) = \\ &= \mathbf{L}(\mathbf{E}) \otimes (\mathbf{E}^{+})\mathbf{L}^{+} = \mathbf{LCL}^{+}, \end{aligned} \tag{1}$$

where $+$ is labelling of the Hermitian conjugate matrix. By decomposition of the coherency matrix of the output optical radiation elements of Stokes vector can be found, enabling description of the fiber sensor features for thermal field disturbance from the point of view optical intensity I.

To determine a coherency matrix of output optical radiation a coherency matrix of input optical radiation and Jones unitary matrix of PMF were needed. For excitation of both polarization axes at any angle of the fiber a clockwise polarized optical radiation was introduced, described by Jones matrix $\mathbf{J}_{\mathrm{RC}}$:

$$\mathbf{J}_{\mathrm{RC}} = \begin{pmatrix} -i \\ 1 \end{pmatrix}. \tag{2}$$

The suffix RC expresses right circular polarization. The coherency matrix of an input optical radiation provides as:

$$\begin{aligned}\mathbf{C} &= \langle \mathbf{E} \otimes \mathbf{E}^{+} \rangle = \left\langle \begin{pmatrix} E_x \\ E_y \end{pmatrix} \otimes \begin{pmatrix} E_x^* & E_y^* \end{pmatrix} \right\rangle = \\ &= \begin{pmatrix} \langle E_x E_x^* \rangle & \langle E_x E_y^* \rangle \\ \langle E_y E_x^* \rangle & \langle E_y E_y^* \rangle \end{pmatrix} = \begin{pmatrix} C_{xx} & C_{xy} \\ C_{yx} & C_{yy} \end{pmatrix}, \end{aligned} \tag{3}$$

where $\mathbf{E}$ is the Jones column matrix (Jones vector) and $\mathbf{E}^{+}$ is its Hermitian conjugate matrix . Equation (2) is expressed by matrix $\mathbf{C}_{\mathrm{ij}}$ to define Eq. (10). After substitution of Eq. (2) we obtain the coherency matrix of circular optical radiation:

$$\mathbf{C}_{\mathrm{RC}} = \begin{pmatrix} -i \\ 1 \end{pmatrix} \otimes \begin{pmatrix} i & 1 \end{pmatrix} = \begin{pmatrix} 1 & -i \\ i & 1 \end{pmatrix}. \tag{4}$$

The phase shift of the linear retarder ϕ is put into the Jones matrix of a linear retarder with azimuth 0 °. By this common relation of linear retarder is obtained as:

$$\mathbf{L} = \begin{pmatrix} e^{i\frac{\phi}{2}} & 0 \\ 0 & e^{-i\frac{\phi}{2}} \end{pmatrix}. \tag{5}$$

Hermitian conjugate matrix to the matrix Eq. (5) can then be expressed as:

$$\mathbf{L}^{+} = \begin{pmatrix} e^{-i\frac{\phi}{2}} & 0 \\ 0 & e^{i\frac{\phi}{2}} \end{pmatrix}. \tag{6}$$

By the substitution of matrices Eq. (4), Eq. (5) and Eq. (6) into Eq. (1) we obtain coherency matrix of output optical radiation:

$$\begin{aligned}\mathbf{C}'_{\mathrm{RC}} &= \mathbf{LC}_{\mathrm{RC}}\mathbf{L}^{+} = \\ &= \begin{pmatrix} e^{i\frac{\phi}{2}} & 0 \\ 0 & e^{-i\frac{\phi}{2}} \end{pmatrix} \begin{pmatrix} 1 & -i \\ i & 1 \end{pmatrix} \begin{pmatrix} e^{-i\frac{\phi}{2}} & 0 \\ 0 & e^{i\frac{\phi}{2}} \end{pmatrix}. \end{aligned} \tag{7}$$

By calculating the matrix product in Eq. (7), a resultant relation of coherency matrix for output optical radiation can be obtained:

$$\mathbf{C}' = \begin{pmatrix} 1 & -ie^{i\phi} \\ ie^{-i\phi} & 1 \end{pmatrix}. \tag{8}$$

By decomposition of Eq. (8) into the spin matrices using the following equation,

$$\begin{aligned}\mathbf{C} &= \frac{C_{xx}+C_{yy}}{2}\begin{pmatrix} 1 & 0 \\ 0 & 1 \end{pmatrix} + \frac{C_{xx}-C_{yy}}{2}\begin{pmatrix} 1 & 0 \\ 0 & -1 \end{pmatrix} + \\ &+ \frac{C_{xy}+C_{yx}}{2}\begin{pmatrix} 0 & 1 \\ 1 & 0 \end{pmatrix} + \\ &+ \frac{C_{xy}-C_{yx}}{2}\begin{pmatrix} 0 & -i \\ i & 0 \end{pmatrix}, \end{aligned} \tag{9}$$

we obtain:

$$\mathbf{C}' = \begin{pmatrix} 1 & 0 \\ 0 & 1 \end{pmatrix} + \sin\phi \begin{pmatrix} 0 & 1 \\ 1 & 0 \end{pmatrix} + \cos\phi \begin{pmatrix} 0 & -i \\ i & 0 \end{pmatrix}. \quad (10)$$

From the relation Eq. (10) it is obvious an assignment of components on the right side of the equation to the corresponding components of Stokes vector. Unit matrix corresponds to the component S_0, the component with multiple $\sin\phi$ corresponds to S_2 and the component with multiple $\cos\phi$ corresponds to S_3. Distribution of optical intensity I in the vertical preference is zero according to the definition $S_1 = C_{xx} - C_{yy}$.

For the length of the optical fiber equaling to the multiple of its beat length and for excitation of both polarization axes by means of circular polarized optical radiation with no disturbance of external thermal field, the phase shift ϕ will be equal to zero and the corresponding Stokes component $S_2 = 0$. For optical fiber length different from a multiple of its beat length and without effect of the external thermal field disturbance the phase shift will be none zero and will be determining the particular state of polarization. In the case of ambient thermal field disturbance by means of an external thermal source the phase shift will be excited and it will result as a change of the output polarization state. This variation of the polarization state is directly proportional to the change of ϕ according to the relation Eq. (11). Determination of this change is realized by means of polarizer - analyzer placed in the output of fiber. For obtaining the maximum sensor sensitivity the orientation of the output polarizer – analyzer is 45 ° towards polarization axes. By this arrangement we can measure the whole range of the phase shift, expressed by the minimum and the maximum value of the measured optical intensity I.

Due to the character of the measured quantity, the optical intensity I, is preferable for next description to use a Mueller matrix. Behavior of the input circular polarized optical radiation propagating through the sensor under consideration, the linear retarder, is expressed by the Mueller matrix as follows:

$$\begin{pmatrix} S_0 \\ S_1 \\ S_2 \\ S_3 \end{pmatrix} = \begin{pmatrix} 1 & 0 & 0 & 0 \\ 0 & 1 & 0 & 0 \\ 0 & 0 & \cos\phi & \sin\phi \\ 0 & 0 & -\sin\phi & \cos\phi \end{pmatrix} \begin{pmatrix} 1 \\ 0 \\ 0 \\ 1 \end{pmatrix} = \begin{pmatrix} 1 \\ 0 \\ \sin\phi \\ \cos\phi \end{pmatrix}. \quad (11)$$

The output optical radiation Eq. (11) hits the linear polarizer – analyzer in the required orientation towards the polarization axes. In the output of polarizer we obtain the optical radiation expressed by the Stokes vector:

$$\begin{pmatrix} S_0' \\ S_1' \\ S_2' \\ S_3' \end{pmatrix} = \frac{1}{2} \begin{pmatrix} 1 & 0 & 1 & 0 \\ 0 & 0 & 0 & 0 \\ 1 & 0 & 1 & 0 \\ 0 & 0 & 0 & 0 \end{pmatrix} \begin{pmatrix} 1 \\ 0 \\ \sin\phi \\ \cos\phi \end{pmatrix} = \frac{1}{2} \begin{pmatrix} 1+\sin\phi \\ 0 \\ 1+\sin\phi \\ 0 \end{pmatrix}. \quad (12)$$

From this resultant equation it is clear that the output optical radiation of the polarizer – analyzer will be linearly polarized with an orientation of 45 ° and the change of optical intensity is directly proportional to the change of phase shift in fiber. From Eq. (12) it is evident that for given arrangement we measured by the photodetector directly the value of Stokes element S_2. Since the variations of phase shift in fiber and development of the polarization state of propagating optical radiation through the fiber, these variations are proportional to the S_2 and S_3 according to Eq. (10). To evaluate these variations we need know only one measured Stokes element S_2' or S_3'. If S_2' is known, S_3' can be calculated. The measured Stokes element S_2' is determined from Eq. (12) as:

$$S_2' = \frac{1}{2}(1+\sin\phi) = \left(\sin\frac{\phi}{2} + \cos\frac{\phi}{2}\right)^2. \quad (13)$$

As we measure optical intensity I of Stokes element S_2' and not a phase shift, we determine ϕ from Eq. (13) as:

$$\phi = \arcsin(2S_2' - 1). \quad (14)$$

Such analysis deals with the description of sensor from the point of view of the outer optical intensity I. In order to describe internal phenomenon in more detail theoretical analysis focusing on the change of the beat length depending upon the temperature variation excited by an external subject was conducted.

3. Phase Shift Variation Depending on Temperature

When studying PM fiber temperature dependency, it can be presumed that the output polarization state variation is dependent on the refractive indices change of fast and slow polarization axes, i.e. the refractive

indices change invoked by a temperature change is proportional to the beat length L_B variation. This is the length where 2π phase shift is introduced between the two polarization axes. The variation of beat length depending upon temperature can be described by the following method. The beat length can be expressed as: [11]

$$L_B = \frac{\lambda}{\Delta n_e}, \tag{15}$$

where λ is the wavelength and Δn_e is the differential index. The differential index is defined as:

$$\Delta n_e = \Delta n_s - \Delta n_f, \tag{16}$$

where Δn_s and Δn_f are differences between refractive indices of particular axes n_s, n_f and the cladding refractive index n_c:

$$\begin{aligned} \Delta n_s &= n_s - n_c, \\ \Delta n_f &= n_f - n_c. \end{aligned} \tag{17}$$

The dependency of beat length variation L_B on Δn_e can be written as:

$$\frac{dL_B}{d\Delta n_e} = -\frac{\lambda}{\Delta n_e^2} = -L_B \frac{1}{\Delta n_e}. \tag{18}$$

Under the condition that phase shift variation δ is linearly dependent on the beat length variation L_B, it can be expressed as:

$$-\frac{d\delta}{2\pi} = \frac{dL_B}{L_B}, \tag{19}$$

where the sign – (minus) indicates the state for which the beat length L_B decreases and the phase shift variation δ increases.

By integration of equation Eq. (19) the following relation is obtained:

$$\delta = -2\pi \int \frac{dL_B}{L_B} = -2\pi(\ln L_B + C). \tag{20}$$

For the ambient temperature the beat length is L_{B0} and the phase shift variation $\delta = 0$. For these conditions the following formula is valid:

$$C = -\ln L_{B0}. \tag{21}$$

By substituting the constant C Eq. (21) into Eq. (20), the phase shift variation shall be:

$$\delta = -2\pi \ln \frac{L_B}{L_{B0}}. \tag{22}$$

By substituting Eq. (15) into Eq. (22), the beat length depending on a differential index Δn_e, phase shift variation can be obtained:

$$\delta = 2\pi \ln \frac{\Delta n_e}{\Delta n_{e0}}, \tag{23}$$

where Δn_{e0} is corresponding to L_{B0}. Under the condition that Δn_e is linearly changing with temperature ϑ, the following formula applies:

$$\Delta n_e(\vartheta - \vartheta_0) = K(\vartheta - \vartheta_0) + \Delta n_{e0}, \tag{24}$$

where K is a proportion constant, ϑ is the excitation source temperature and ϑ_0 is the ambient temperature. The phase shift variation dependence on temperature is then expressed by substituting Eq. (24) into Eq. (23):

$$\delta(\vartheta - \vartheta_0) = 2\pi \ln \left(\frac{K(\vartheta - \vartheta_0)}{\Delta n_{e0}} + 1 \right). \tag{25}$$

The phase shift variation dependence on temperature expressed in Eq. (25) is valid on condition that the difference of refractive indices of fast and slow axes is proportional to the temperature. The resultant PM fiber response is dependent on the number of exposed beat lengths the heat source is affecting. The response is different due to the constant source length and different beat lengths of particular PM fibers. Therefore it is suitable to consider PM fiber responses related only to one beat length. The total phase shift variation δ dependence on the total number of exposed beat lengths and the phase shift variation δ_{LB} dependence on one beat length is expressed by the following formula, where N is the number of exposed beat lengths L_B effected by the heat source:

$$N = \frac{l}{L_B}, \tag{26}$$

where l is the exposed length of PM fiber. As the heat source effect at the ends is not defined exactly the number N can be rounded to an integer number. The phase shift variation of one beat length δ_{LB} is expressed as:

$$\delta_{LB} = \frac{\delta}{N} = \delta \frac{L_B}{l}. \tag{27}$$

For a differential index the following formula is valid:

$$\Delta n_e = \frac{\lambda}{L_B}. \tag{28}$$

Tab. 1: Features of PM fibers.

Type of OF	Wavelength [nm]	Beat length L_B [mm]	Δn_e $[\times 10^{-3}]$	Factor L_B/l $[\times 10^{-3}]$
PM630-HP	633	2	0.316	7.2
PM1300-HP	1310	4	0.327	14.5
PM1550-HP	1550	5	0.31	18

Tab. 2: Phase shift variation per one beat length for fiber PM630-HP.

Phase shift variation per one beatlength					
		Temperature source distance from PMF			
		5 [cm]	8 [cm]	11 [cm]	
Temp.	50 °C	13.00	12.00	8.90	$\pi \times 10^{-3}$ $[rad]$
	45 °C	10.90	8.20	7.10	
	40 °C	7.70	6.80	5.30	
	35 °C	5.70	4.70	2.90	

Factors L_B/l and differential refractive index values Δn_e of particular PM fibers are presented in Tab. 1. In the case there is m mumber of exposed lengths of PMF the value of the factor shall be L_B/ml. The differential indices Δn_e of studied PM fibers are practically the same and that the difference of refractive indices between fast and slow axes and mechanism of birefringence generation is very similar for all the selected PM fibers. This conclusion is supported by the production technology of identical producer during industrial process of PANDA structures of particular PM fibers. The temperature response related to the one beat length should be literally the same.

A coefficient for determining sensitivity per beat length for length $l = 27.5$ cm is presented in Tab. 1. The length l is corresponding to the length of the applied heat source.

4. Experimental Results

The aim of our experimental tests is to determine PM fiber PANDA type response during its thermal field disturbance when an external thermal source with different initial temperatures was applied. The temperature was changed from 50 °C to 35 °C in 5 °C steps. Measurements were taken for two different exposed fiber lengths. The fiber response was investigated for three different distances (5 cm, 8 cm and 11 cm) between the thermal source and the optical fiber. Disturbance of the thermal PM fiber field was done using a plastic basin with a constant amount of water heated to the desired temperature. It was placed on a gap between 2 polystyrene boards Fig. 1 that cover the unexposed part of the PMF.

The above layout in the sensor block enables the exposition of the required length of investigated fiber and

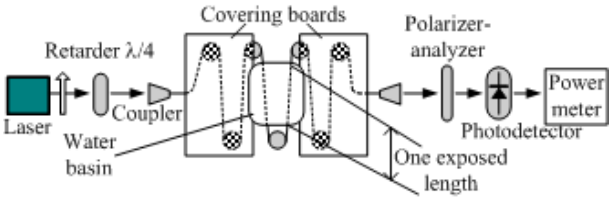

Fig. 1: Test setup for measuring two exposed lengths [9].

also enables to arrange the required distance of ambient thermal field from the fiber. In this experiment, a fiber response for 1 and 3 exposed lengths were tested between cork cylinders. One exposed length was 27.5 cm. The source of optical radiation used for $\lambda = 633$ nm was He-Ne laser, for $\lambda = 1310$ nm and 1550 nm laser diodes ML 725 B8F and ML 925 B45F, respectively, were used.

The beat length catalogue value of fiber PM630-HP is $L_B \leq 2$ mm, for PM1300-HP is $L_B \leq 4$ mm and for PM1550-HP is $L_B \leq 5$ mm. Optical power for $\lambda = 1310$ nm and 1550 nm was measured in intervals of 0.5 s using a GENTEC-EO P-LINK power meter with a PH78-Ge photodiode. For $\lambda = 633$ nm, an analog power meter in combination with a HP 34401A digital multimeter was used controlled by MATLAB. The interval for taking these readings was 0.64 s.

Figure 2 shows an example of measured polarization state in the above described given configuration.

For easier illustration and computer modeling of development of the output polarization state, the Poincare sphere [12], [13] was created in the MATLAB environment. The polarization state in Fig. 2 for 1550 nm is depicted on Poincaré sphere in Fig. 3.

The measured results were processed in two graphs versions of phase shift, as a dependency on temperature for different distances between the thermal source and

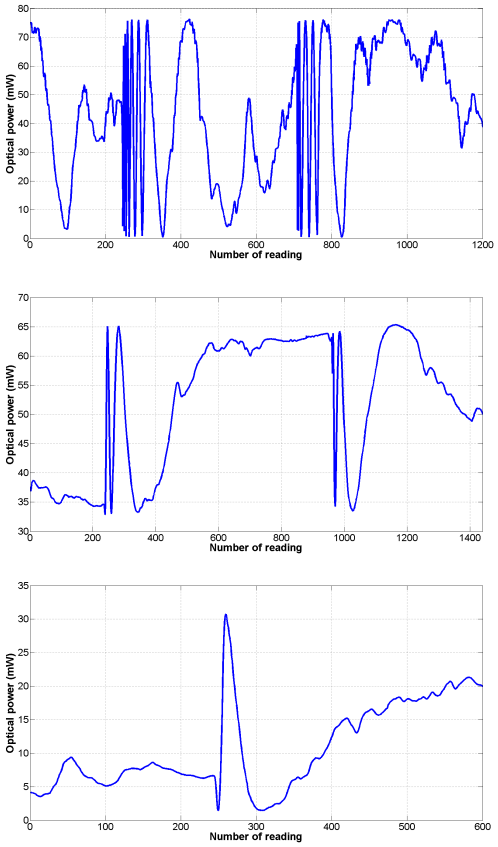

Fig. 2: Example of output optical power for $\lambda = 1310$ nm, 1310 nm and 1550 nm, 3 exposed lengths of fiber, initial temperature 50 °C and 5 cm distance between the external thermal source and the PM fiber.

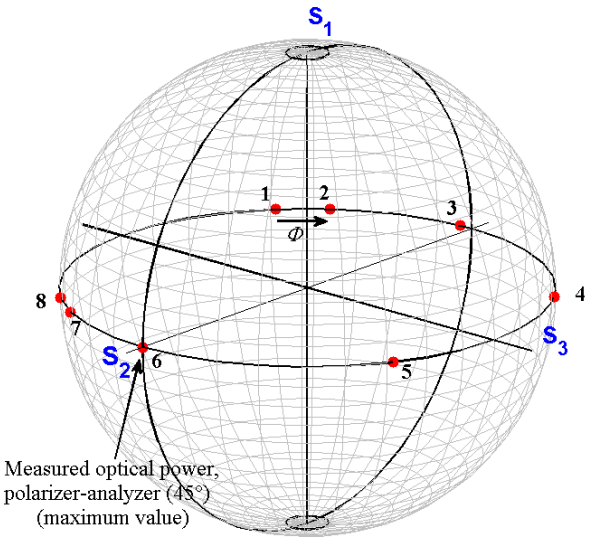

Fig. 3: Polarization state readings of the output optical radiation corresponding to the Fig. 2 at 1550 nm.

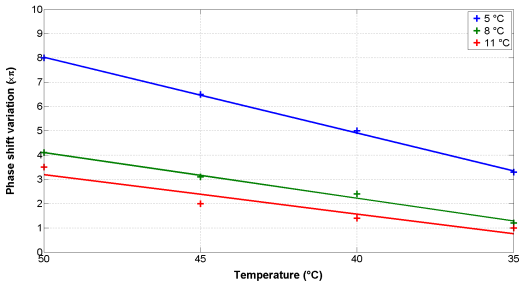

Fig. 4: Phase shift variation dependency on temperature for one exposed length of winding for PM630-HP.

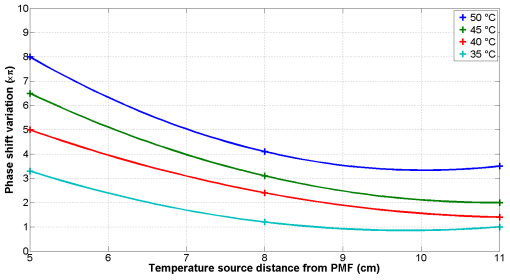

Fig. 5: Phase shift variation dependency on the distance of thermal source from PM fiber for one exposed length of winding for PM630-HP.

the fiber and as a dependency on the distance for the selected temperatures. The presented approximations come from readings at temperatures of 50 °, 45 °, 40 ° and 35 ° and at distances of 5 cm, 8 cm and 11 cm. Examples of these distances for one exposed length are shown in Fig. 4, Fig. 5, Fig. 8, Fig. 9, Fig. 12 and Fig. 13, results for three exposed lengths are in Fig. 6, Fig. 7, Fig. 10, Fig. 11, Fig. 14 and Fig. 15.

Fig. 4 and Fig. 6 show that dependencies of phase shift variation on the temperature are approximately linear. Similarly with increasing exposed length the phase shift variation increases too, but slowly. There was only one anomaly presented at the distance of 5 cm, where a big value of phase shift variation was caused by the thermal source affecting also the neighboring lengths of the fiber that were not supposed to be exposed.

Examples of the phase shift variation dependence on the distance for selected temperatures are shown in Fig. 5 and Fig. 7. Nonlinearity of the dependency for one exposed length validates the fact that for shorter distances and greater temperature emission of thermal source there are undesired interferences, effecting other than the required exposed length. This heat effect is substantially smaller in the case of three exposed lengths, as the undesired coverage of effected lengths is smaller. The presented examples are a part of a large set of measurements for sensitivity tests depending on the fiber configuration and the ambient temperature.

One of the aims of this study is to compare thermal field disturbance for three PM fibers working atn different wavelengths of 633 nm, 1310 nm and 1550 nm. As

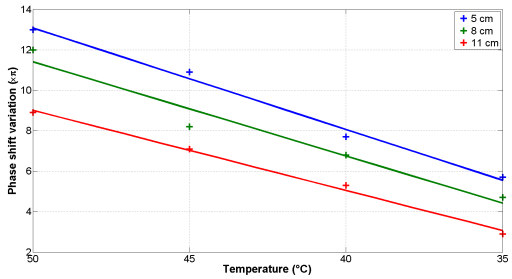

Fig. 6: Phase shift variation dependence on temperature for three exposed lengths of winding for PM630-HP.

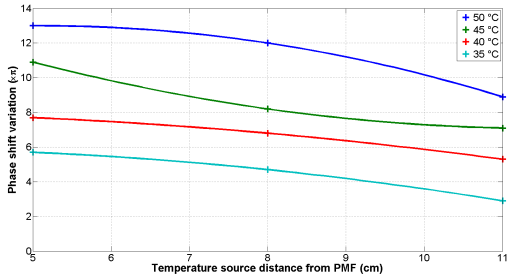

Fig. 7: Phase shift variation dependence on distance between thermal source and PM fiber for three exposed lengths of winding for PM630-HP.

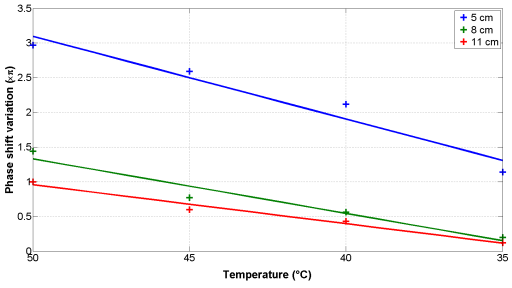

Fig. 8: Phase shift variation dependence on temperature for one exposed length of winding for PM1300-HP.

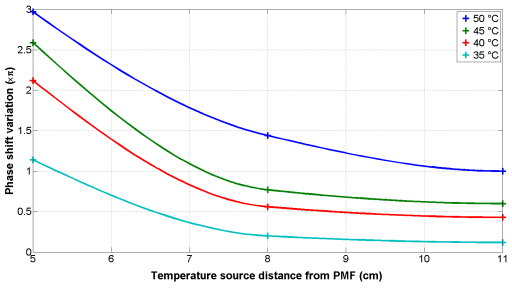

Fig. 9: Phase shift variation dependence on distance between thermal source and PM fiber for one exposed length of winding for PM1300-HP.

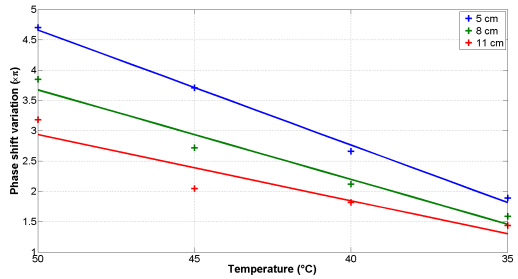

Fig. 10: Phase shift variation dependence on temperature for three exposed lengths of winding for PM1300-HP.

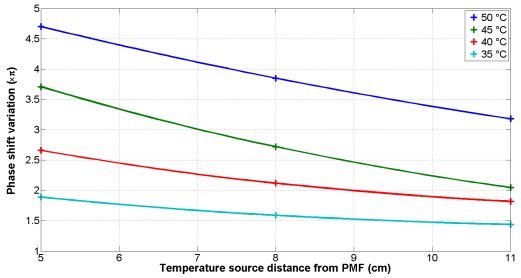

Fig. 11: Phase shift variation dependence on distance between thermal source and PM fiber for three exposed lengths of winding for PM1300-HP.

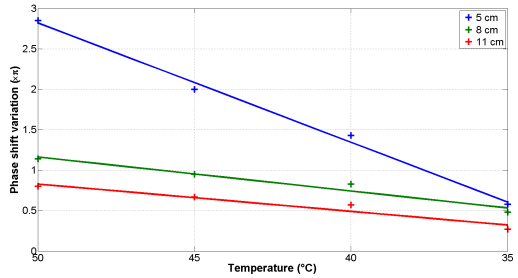

Fig. 12: Phase shift variation dependence on temperature for one exposed length of winding for PM1550-HP.

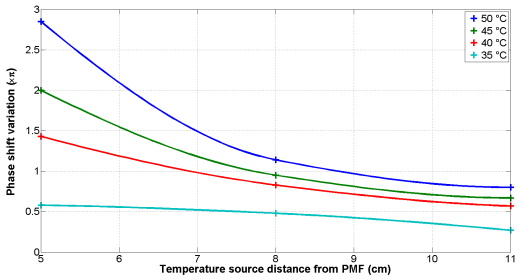

Fig. 13: Phase shift variation dependence on distance between thermal source and PM fiber for one exposed length of winding for PM1550-HP.

the phase shift variation δ is dependent on the number of beat lengths, the measured responses were recalculated according to Eq. (27). Obtained results for particular PM fibers are presented in Tab. 2, Tab. 3 and Tab. 4.

Tab. 3: Phase shift variation per one beat length for fiber PM1330-HP.

Phase shift variation per one beatlength					
		Temperature source distance from PMF			
		5 [cm]	8 [cm]	11 [cm]	
Temp.	50 °C	4.70	3.85	3.18	$\pi \times 10^{-3}$ $[rad]$
	45 °C	3.71	2.72	2.05	
	40 °C	2.66	2.12	1.82	
	35 °C	1.89	1.56	1.44	

Tab. 4: Phase shift variation per one beat length for fiber PM1550-HP.

Phase shift variation per one beatlength					
		Temperature source distance from PMF			
		5 [cm]	8 [cm]	11 [cm]	
Temp.	50 °C	2.85	1.14	0.80	$\pi \times 10^{-3}$ $[rad]$
	45 °C	2.00	0.95	0.67	
	40 °C	1.43	0.83	0.57	
	35 °C	0.58	0.48	0.27	

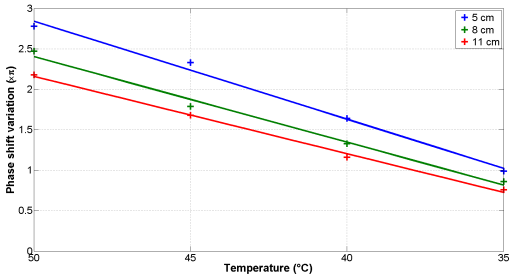

Fig. 14: Phase shift variation dependence on temperature for three exposed lengths of winding for PM1550-HP.

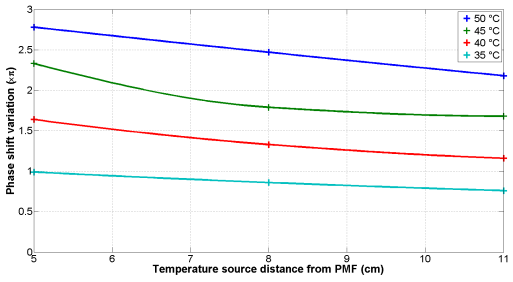

Fig. 15: Phase shift variation dependence on distance between thermal source and PM fiber for three exposed lengths of winding for PM1550-HP.

All measurements show relatively high instability and sensitivity to other surrounding effects such as random temperature changes, mechanical vibrations etc. Therefore this application is suitable as a sensor of thermal field disturbance, but not as a precision temperature sensor. High sensitivity to temperature changes could be combined with suitable fiber configuration to get the sensitivity to mechanical vibrations, Such sensor applications could be used for territory monitoring, to prevent undesired objects approaching, etc.

5. Conclusion

The presented results complete the tests from a previous study for $\lambda = 633$ nm. By comparing these results, the expected conclusion can be stated, that there is a higher sensitivity for $\lambda = 633$ nm, mainly due to the short beat length and high coherency of the He-Ne laser source. To reach comparable sensitivity at 1550 nm a longer segment of the exposed fiber should be used. As advantage of LD for 1550 nm is the compact set up of the source-fiber-polarizer-detector.

The next study should focus on a detailed analysis of the effect of source coherency on the fiber behavior in respect to a phase shift variation during thermal field disturbance. Generally, also analysis of phase shift variation in time during all the transformations stages could be very interesting, first the initial absorption of the thermal radiation, then successive temperature stabilizing and then transition into a new stable state. Based on this, a compact solutions could be built to be utilized in other practical applications.

Acknowledgment

This work has been supported by Project for the development of K217 Department, Brno University of Defense – Modern electrical elements and systems.

References

[1] PERLICKI, K. Identification of Polarization configuration based on torsion and Curvature Calculation. *WSEAS Transactions of Communications*. 2006, vol. 5, iss. 4, pp. 631–633. ISSN 1109-2742.

[2] VLCEK, C. Study of external effects on the polarization properties of selected fiber segments. *WSEAS Transactions on Communications*. 2006, vol 5, iss. 4, pp. 611–616. ISSN 1109-2742.

[3] MARTELLUCCI, S., A. N. CHESTER and A. G. MIGNANI. *Optical sensors and microsystems, new concepts, materials, technologies*. New York: Kluwer Academic Publishers, 2000. ISBN 978-0306463808.

[4] FRADEN, Jacob. *Handbook of modern sensors: physics, designs, and applications*. New York: Springer, 2010. ISBN 978-1-4419-6465-6.

[5] HOTATE, K. and S. O. S. LENG. Transversal force sensor using polarization-maintaining fiber independent of direction of applied force: proposal and experiment. In: *15th Optical Fiber Sensors Conference Technical Digest. OFS 2002*. Portland: IEEE, 2002, pp. 363–366. ISBN 0-7803-7289-1. DOI: 10.1109/OFS.2002.1000586.

[6] ZHANG, F. and J. W. Y. LIT. Temperature sensitivity measurements of high-birefringent polarization-maintaining fibers. *Applied Optics*. 1993, vol. 32, iss. 13, pp. 2213–2218. ISSN 1559-128X.

[7] DVORAK, F., J. MASCHKE and C. VLCEK. Fiber sensor of temperature field disturbance. In: *4th International Conference on Circuits, Systems and Signal (CSS'10)*. Corfu: World Scientific and Engineering Academy and Society, 2010, pp. 134–139. ISBN 978-960-474-208-0.

[8] DVORAK, F., J. MASCHKE and C. VLCEK. Utilization of birefringent fiber as sensor of temperature field disturbance. *Radioengineering*. 2009, vol. 18, no. 4, pp. 639–643. ISSN 1210-2512.

[9] DVORAK, F., J. MASCHKE and C. VLCEK. Response analysis of thermal field disturbance sensor. In: *Electro-Optical and Infrared Systems: Technology and Applications VIII*. Prague: SPIE, 2011, pp. 501–508. ISBN: 978-081948813-8. DOI: 10.1117/12.897707.

[10] DVORAK, F., J. MASCHKE and C. VLCEK. Study of fiber PM1550-HP response in the set of thermal field disturbance sensor. In: *Proc. of NAUN International Multi-conference, Recent Researchers in Circuits, Systems, Communications & Computers*. Puerto De La Cruz: WSEAS, 2011. pp. 137–141. ISBN 978-1-61804-056-5.

[11] COLLETT, Edward. *Polarized light in fiber optics*. Lincroft: The PolaWave Group, 2003. ISBN 978-081-9457-615.

[12] COLLETT, E. and B. SCHAEFER. Visualization and calculation of polarized light. I. The polarization ellipse, the Poincaré sphere and the hybrid polarization sphere. *Applied optics*. 2008, vol. 47, iss. 22. ISSN 1559-128X. DOI: 10.1364/AO.47.004009.

[13] COLLETT, E. and B. SCHAEFER. Visualization and calculation of polarized light. II. Applications of the hybrid polarization sphere. *Applied optics*. 2008, vol. 47, iss. 22. ISSN 1559-128X. DOI: 10.1364/AO.47.004017.

About Authors

Filip DVORAK was born in 1977. He received his M.Sc. degree from the Brno Military Academy in 2004 and Ph.D. degree in 2011. He is currently lecturer with the Department of Radar Technology, Brno University of Defense. His work is focused on the modeling of fibers and optical components by means of matrix methods in the MATLAB environment and analysis of fiber sensors.

Jan MASCHKE was born in 1942. He received his M.Sc. degree in 1965 and Ph.D. degree in 1978. He was a teacher at the Technical school at Liptovský Mikulas and at the Military Academy since 1968, and associate professor of the Department of electrical engineering since 1985. He retired in 2005. His research work focused on the problems of fiber optics and fiber sensors.

Cestmir VLCEK was born in 1946. He received his M.Sc. degree in 1969 and Ph.D. degree in 1980. He was a teacher at the Military Academy since 1969, associate professor since 1985, head of the Electrical Engineering and Electronics Department since 1997 and professor since 2000. His research work during the last years was aimed at problems of optoelectronic signals and systems, single mode fiber components modeling, atmospheric optical communication systems and analysis of sensors for military applications.